Published in final edited form as:
Adv Mater. 2008 November 3; 20(21): 4154–4157. doi:10.1002/adma.200800756.

Bioinspired Surface Immobilization of Hyaluronic Acid on Monodisperse Magnetite Nanocrystals for Targeted Cancer Imaging**

Yuhan Lee,
Department of Biological Sciences, Korea Advanced Institute of Science and Technology, Daejeon 305-701 (Korea)

Haeshin Lee,
Department of Biomedical Engineering, Northwestern University, Evanston, Illinois 60208 (USA)

Young Beom Kim,
Division of Electrical Engineering, School of Electrical Engineering and Computer Science, Korea Advanced Institute of Science and Technology, Daejeon 305-701 (Korea)

Jaeyoon Kim,
School of Chemical and Biological Engineering, Seoul National University, Seoul 151-744 (Korea)

Taeghwan Hyeon,
School of Chemical and Biological Engineering, Seoul National University, Seoul 151-744 (Korea)

HyunWook Park,
Division of Electrical Engineering, School of Electrical Engineering and Computer Science, Korea Advanced Institute of Science and Technology, Daejeon 305-701 (Korea)

Phillip B. Messersmith, and
Department of Biomedical Engineering, Northwestern University, Evanston, Illinois 60208 (USA)

Tae Gwan Park
Department of Biological Sciences, Korea Advanced Institute of Science and Technology, Daejeon 305-701 (Korea)

Inorganic nanocrystals have attracted much attention for therapeutic and diagnostic applications due to their unique optical, magnetic, and fluorescent properties.[1] Among these various nanocrystals, colloidal superparamagnetic iron oxide (e.g., γ-Fe_2O_3 and Fe_3O_4) have been extensively highlighted for many biomedical applications such as contrast agents for magnetic-resonance (MR) imaging, therapeutic gene carriers, protein purification, and sensors for nucleic-acid and virus detection.[2] In principle, it is of utmost importance to prepare highly stable magnetic nanocrystals in aqueous solutions to maximize in vivo half-life and tissue-specificity. However, the fabrication of such stable, bioactive magnetic nanocolloids has proven to be nontrivial.

Methods for hydrophilic surface modification include addition of surface-active small molecules or polymeric stabilizers[3] and synthesis of magneto-composites via encapsulation.

**This work was supported by the National Research Laboratory program from the Ministry of Science and Technology, Republic of Korea. Supporting Information is available online from Wiley InterScience or from the authors.

E-mail: tgpark@kaist.ac.kr.

[4] The encapsulation approaches involve laborious multistep reactions, and the additional nonmagnetic coatings result in adverse effects on the magnetic properties of the resultant nanoparticles. On the other hand, nanocrystals coated with surface stabilizers often show only short-term stability, and are easily aggregated by slight disruptions in the chemical environments. Thus, the development of simple, robust routes for surface immobilization of bioactive or bioinert molecules onto iron oxide nanocrystals can be useful tools of practical utility in nanomedicine.

Inspired by adhesive proteins secreted by marine mussels (*Mytilus edulis*), we herein report the facile, biomimetic functionalization of hyaluronic acid (HA) with dopamine for stable immobilization onto magnetite-nanocrystal surfaces (HA-DN/MNC). 3,4-dihydroxy-L-phenylalanine (DOPA) is found in mussel specialized adhesive proteins, and is particularly abundant in the proteins found at the interface between adhesive pads and opposing surfaces.[5] A key feature of DOPA and its analog dopamine is the ortho-dihydroxyphenyl (catechol) functional group, which forms strong bonds with various inorganic/organic surfaces that were shown to be stronger than biotin-streptavidin interactions.[6] Recently, dopamine self-polymerization was discovered as a powerful approach to applying multifunctional coatings onto many surfaces, including noble metals, metal oxides, ceramics, and polymers.[6b] Although the dopamine moiety has been previously utilized for surface modification of various nanoparticles with PEG and other ligands,[7] bioactive targeting macromolecules such as HA have never been immobilized on the surface of magnetite nanocrystals for cancer-cell imaging.

HA, one of the major components of vertebrate tissue and body fluid, has been known to interact with the hyaluronan receptor, CD44. HA-CD44 binding triggers intracellular signals that influence cellular proliferation, differentiation, and migration. It is also known that CD44 overexpression is associated with cancerous angiogenesis and other types of tumor progression.[8] As a result, HA has been utilized as a targeting ligand in various nanomedicine studies directed to cancer cells. Thus, the surface immobilization of HA onto iron oxide nanocrystals is a promising method to target tumor cells. At the same time, the superparamagnetic property of these particles allows for tumor-tissue imaging.

Monodisperse magnetite nanocrystals with an average size of 12 nm were synthesized using thermal decomposition of iron oleate complex, as previously reported.[9] For HA surface immobilization, the nanocrystals were transferred to an aqueous phase using cetyltrimethylammonium bromide (CTAB), which provided cationic properties to the surface, facilitating electrostatic interactions with negatively charged HA, as described in Scheme 1.[10] CTAB is known to form an interdigitated bilayer structure on alkane-terminated metallic-nanocrystal surfaces.[10b] HA-dopamine conjugates (HA-DN) were prepared using conventional 1-ethyl-3-(3-dimethylaminopropyl) carbodiimide hydrochloride (EDC)/1-hydoxybenzotriazole (HOBT) chemistry in pH 5.5 solution to avoid irreversible oxidation of dopamine.[6b] The degree of dopamine substitution in HA determined by ^{1}H-NMR was 41.4%. The homogeneous coating with HA-DN was achieved by adding a solution of nanocrystals into the HA-DN solution with vortexing for 1 min. As shown in Scheme 1, fast electrostatic interactions between positive-charged MNC surface and negative-charged HA-DN might induce such an instantaneous surface coating in aqueous solution. Unbound CTAB and HA-DN molecules were removed by centrifugation of the HA-DN/MNC complexes (see Supporting Information for the detailed procedure).

Atomic force microscopy (AFM) images clearly show the homogeneous coating of HA-DN on the surface of the magnetite nanocrystals (Fig. 1a and b). Particles dispersed on a mica surface revealed that the average height ((15.2 ± 0.4) nm) was increased by 1.6 nm compared to the diameter of uncoated nanocrystals ((12 ± 0.1) nm) (Fig. 1c). High-resolution X-ray photoelectron spectra (N 1s orbital) confirmed the presence of HA-DN; the binding energy of

the quaternary nitrogen in CTAB (403.2 eV) was different from that of nitrogens in N-acetyl and amide groups in HA-DN (Scheme 1, 401.2 eV and 399.8 eV, respectively), indicating the replacement of CTAB with HA-DN (see Fig. S1 in Supporting Information). Transmission electron microscopy (TEM) analysis along with control experiments using SDS-modified nanocrystals revealed that the surface charge of the nanocrystals is crucial for good colloidal dispersion. For example, SDS-modified (e.g., negatively charged) nanocrystals tend to aggregate along the contour length of the HA-DN chain (see Fig. S2 in Supporting Information), whereas interactions between CTAB-modified nanocrystals and HA-DN consistently yielded well-dispersed HA-DN-coated nanoparticles (Fig. 1d). These TEM results (individual vs. aggregate) suggest that HA-DN molecules were initially attracted by electrostatic interactions, with the catechol groups subsequently forming stable chemical bonds on the nanocrystal surface, resulting in the formation of HA-DN/MNC complexes.

To investigate the effect of coatings on their magnetic properties, as-prepared and HA-DN-modified nanocrystals were analyzed using a superconducting quantum interference device (SQUID) at 260 K. Both magnetite nanocrystals exhibited superparamagnetic properties, as indicated by the absence of a hysteresis loop (Fig. 1e), and the reduction of the saturation magnetization value (*Ms*) was marginal (~33%, $Ms_{\gamma\text{-}Fe_2O_3}$ = 12 emu g^{-1}, $Ms_{HA\text{-}DN/MNC}$ = 8 emu g^{-1}), indicating that noncollinear spins were only slightly influenced by the surface coat of HA-DN (~1.6 nm in thickness).[11] Such a small reduction in magnetization is also promising for biomedical applications such as magnetofection and magnetic drug delivery.[10a]

Long-term stability in water and high-concentration salt buffer solutions was observed, for potential in vivo imaging applications. As shown in Figure 1f, HA-DN/MNCs exhibited excellent stability in aqueous solutions, showing no apparent precipitation for 4 days. In contrast, CTAB-stabilized nanocrystals transferred to distilled water or HA solution were agglomerated and entirely precipitated after a short period of time (1 h and 3 h, respectively, Fig. 1f). These results may be attributed to desorption of CTAB molecules from the nanocrystal surface resulting in aggregation, as shown in AFM images (Fig. S3). In addition, the degree of dopamine conjugation in the HA chain dictated the colloidal stability of HA-DN/MNC complexes, as shown in Figure 1f columns 3 (HA-DN-L, ~17.0%: 7 mol DN/mol HA) and 4 (HA-DN, 41.4%: ~17 mol DN/mol HA). HA-DN with greater dopamine substitution resulted in greatly enhanced stability compared to HA-DN-L. HA-DN/MNCs also showed great stability under physiological conditions (pH 7.4 Phosphate buffered saline (PBS) solution), suggesting promise for in vivo applications.

To test the diagnostic effectiveness of HA-DN/MNCs, T_2-weighted gradient-echo MR imaging (3 tesla) was performed using CD44+ cells (HCT116, human colon carcinoma cell line), and CD44-fibroblast cells (NIH3T3, mouse fibroblast) as a control. The MR imaging revealed that the cellular uptake of HA-DN/MNC was greatly enhanced in HCT116 by specific CD44-HA receptor-ligand interactions (Fig. 2a). The difference in relative relaxation rates, R_2, ($= \Delta R_2 / R_{2cont.}$; $R_2 = T_2^{-1}$) between HA-DN/MNC-treated and nontreated cells was 26% for HCT116 and 7% for NIH3T3 cells (Fig. 2b).

The increased cellular uptake to HCT116 cells (3.7 times) was further verified using Prussian blue assay, which detected the amount of iron oxide nanocrystals. It was observed that MNCs coated with HA molecules that were not conjugated with dopamine (HA/MNC) exhibited a low degree of cellular uptake, regardless of tested cell lines, presumably because of HA desorption (left, Fig. 2c). In contrast, the cellular uptake of HA-DN/MNCs within HCT116 cells was greatly enhanced compared to that observed in NIH3T3 (right, Fig. 2c). Furthermore, the ligand competition experiment performed in the presence of excess HA in the culture medium demonstrated effective suppression of HA-DN/MNC cellular uptake to the level of

NIH3T3 cells, revealing that the mechanism for intracellular delivery of HA-DN/MNCs was a CD44-mediated, receptor-mediated endocytosis. Thus, the conjugation of dopamine to the HA chain and the subsequent anchoring of HA-DN on the surface of MNCs via bioinspired adhesion played a pivotal role in target-specific enhanced MR imaging and cellular uptake for tumor cells. The present surface-immobilization technique provides a facile route for systemic delivery of MR contrast agents for tumor targeting.

In conclusion, we reported a mussel-inspired method for homogeneous and robust coating of HA on monodisperse magnetite nanocrystals in aqueous solution with a cancer targeting capability via CD44-HA receptor-ligand interactions.

Experimental

See Supporting Information for the detailed experimental procedure.

References

[1]. a) Alivisatos P. Nat. Biotechnol 2004;22:47. [PubMed: 14704706] b) Storhoff JJ, Mirkin CA. Chem. Rev 1999;99:1849. [PubMed: 11849013] c) Lee J, Hernandez P, Lee J, Govorov AO, Kotov NA. Nat. Mater 2007;6:291. [PubMed: 17384635] d) Lee J, Javed T, Skeini T, Govorov AO, Bryant GW, Kotov NA. Angew. Chem 2006;118:4937.Angew. Chem. Int. Ed 2006;45:4819. e) Nam KT, Kim D-W, Yoo PJ, Chiang C-Y, Meethong N, Hammond PT, Chiang Y-M, Belcher AM. Science 2006;312:885. [PubMed: 16601154] f) Niemeyer CM. Angew. Chem 2001;113:4254.Angew. Chem. Int. Ed 2001;40:4128. g) Medintz IL, Uyeda HT, Goldman ER, Mattoussi H. Nat. Mater 2005;4:435. [PubMed: 15928695] h) Gu H, Xu K, Xu C, Xu B. Chem. Commun 2006;941

[2]. a) Mirkin CA, Letsinger RL, Mucic RC, Storhoff JJ. Nature 1996;382:607. [PubMed: 8757129] b) Oh BK, Nam J-M, Lee SW, Mirkin CA. Small 2006;2:103. [PubMed: 17193564] c) Choi J-S, Jun Y-W, Yeon S-I, Kim HC, Shin J-S, Cheon J. J. Am. Chem. Soc 2006;128:15982. [PubMed: 17165720] d) Lee IS, Lee N, Park J, Kim BH, Yi Y-W, Kim T, Kim TK, Lee IH, Paik SR, Hyeon T. J. Am. Chem. Soc 2006;128:10658. [PubMed: 16910642] e) Perez JS, Simeone FJ, Saeki Y, Josephson L, Weissleder R. J. Am. Chem. Soc 2003;125:10192. [PubMed: 12926940] f) Josephson L, Perez JM, Weissleder R. Angew. Chem 2001;113:3304.Angew. Chem. Int. Ed 2001;40:3204.

[3]. a) Huh Y-M, Jun Y, Kim S, Choi J, Lee J-H, Yoon S, Kim K-S, Shin J-S, Suh S-J, Cheon J. J. Am. Chem. Soc 2005;127:12387. [PubMed: 16131220] b) Wagner K, Kautz A, Roder M, Schwalbe M, Pachmann K, Clement JH, Schnabelrauch M. Appl. Organomet. Chem 2004;18:514. c) Robinson DB, Persson HH, Zeng H, Li G, Pourmand N, Sun S, Wang SX. Langmuir 2005;21:3096. [PubMed: 15779990] d) Zhang Z, Kohler N, Zhang M. Biomaterials 2002;23:1553. [PubMed: 11922461] e) Susumu K, Uyeda HT, Medintz IL, Pons T, Delehanty JB, Mattoussi H. J. Am. Chem. Soc 2007;129:13987. [PubMed: 17956097]

[4]. a) Yang J, Lee C-H, Ko H-J, Suh J-S, Yoon H-G, Lee K, Huh Y-M, Haam S. Angew. Chem 2007;119:8992.Angew. Chem. Int. Ed 2007;46:8836. b) Stoeva SI, Huo F, Lee J-S, Mirkin CA. J. Am. Chem. Soc 2005;127:15362. [PubMed: 16262387]

[5]. Waite JH, Qin XX. Biochemistry 2001;40:2887. [PubMed: 11258900]

[6]. a) Lee H, Scherer NF, Messersmith PB. Proc. Natl. Acad. Sci. USA 2006;103:12999. [PubMed: 16920796] b) Lee H, Dellatore SM, Miller WM, Messersmith PB. Science 2007;318:426. [PubMed: 17947576] c) Lee H, Lee BP, Messersmith PB. Nature 2007;448:338. [PubMed: 17637666]

[7]. a) Xie J, Xu C, Xu Z, Hou Y, Young KL, Wang SX, Pourmand N, Sun S. Chem. Mater 2006;18:5401. [PubMed: 18176627] b) Xu C, Xu K, Gu H, Zheng R, Liu H, Zhang X, Guo Z, Xu B. J. Am. Chem. Soc 2004;126:9938. [PubMed: 15303865] c) Wang L, Yang Z, Gao J, Xu K, Gu H, Zhang B, Zhang X, Xu B. J. Am. Chem. Soc 2006;128:13358. [PubMed: 17031939] d) Xu C, Xie J, Ho D, Wang C, Kohler N, Walsh EG, Morgan JR, Chin YE, Sun S. Angew. Chem. Int. Ed 2008;47:173. e) Shultz MD, Reveles JU, Khanna SN, Carpenter EE. J. Am. Chem. Soc 2007;129:2482. [PubMed: 17290990]

[8]. a) Lapcik L Jr, Lapcik L, Smedt SD, Demeester J, Chabrecek P. Chem. Rev 1998;98:2663. [PubMed: 11848975] b) Lee JY, Spicer AP. Curr. Opin. Cell Biol 2000;12:581. [PubMed: 10978893] c) Collis

L, Hall C, Lange L, Ziebell M, Prestwich R, Turley EA. FEBS Lett 1998;440:444. [PubMed: 9872419] d) Watanabe H, Yamada Y. Nature Genet 1999;21:225. [PubMed: 9988279] e) Luo Y, Prestwich D. Bioconjugate Chem 1999;10:755. f) Mok H, Park JW, Park TG. Bioconjugate Chem 2007;18:1483. g) Lee H, Mok H, Lee S, Oh Y, Park TG. J. Controlled Release 2007;119:245.

[9]. Park J, An K, Hwang Y, Park J-G, Noh H-J, Kim J-Y, Park J-H, Hwang N-M, Hyeon T. Nat. Mater 2004;3:891. [PubMed: 15568032]

[10]. a) Kim J, Lee JE, Lee J, Yu JH, Kim BC, An K, Hwang Y, Shin C-H, Park J-G, Kim J, Hyeon T. J. Am. Chem. Soc 2006;128:688. [PubMed: 16417336] b) Fan H, Yang K, Boye DM, Sigmon T, Malloy KJ, Xu H, Lopez GP, Brinker CJ. Science 2004;304:567. [PubMed: 15105495]

[11]. Hu F, Neoh KG, Cen L, Kang E-T. Biomacromolecules 2006;7:809. [PubMed: 16529418]

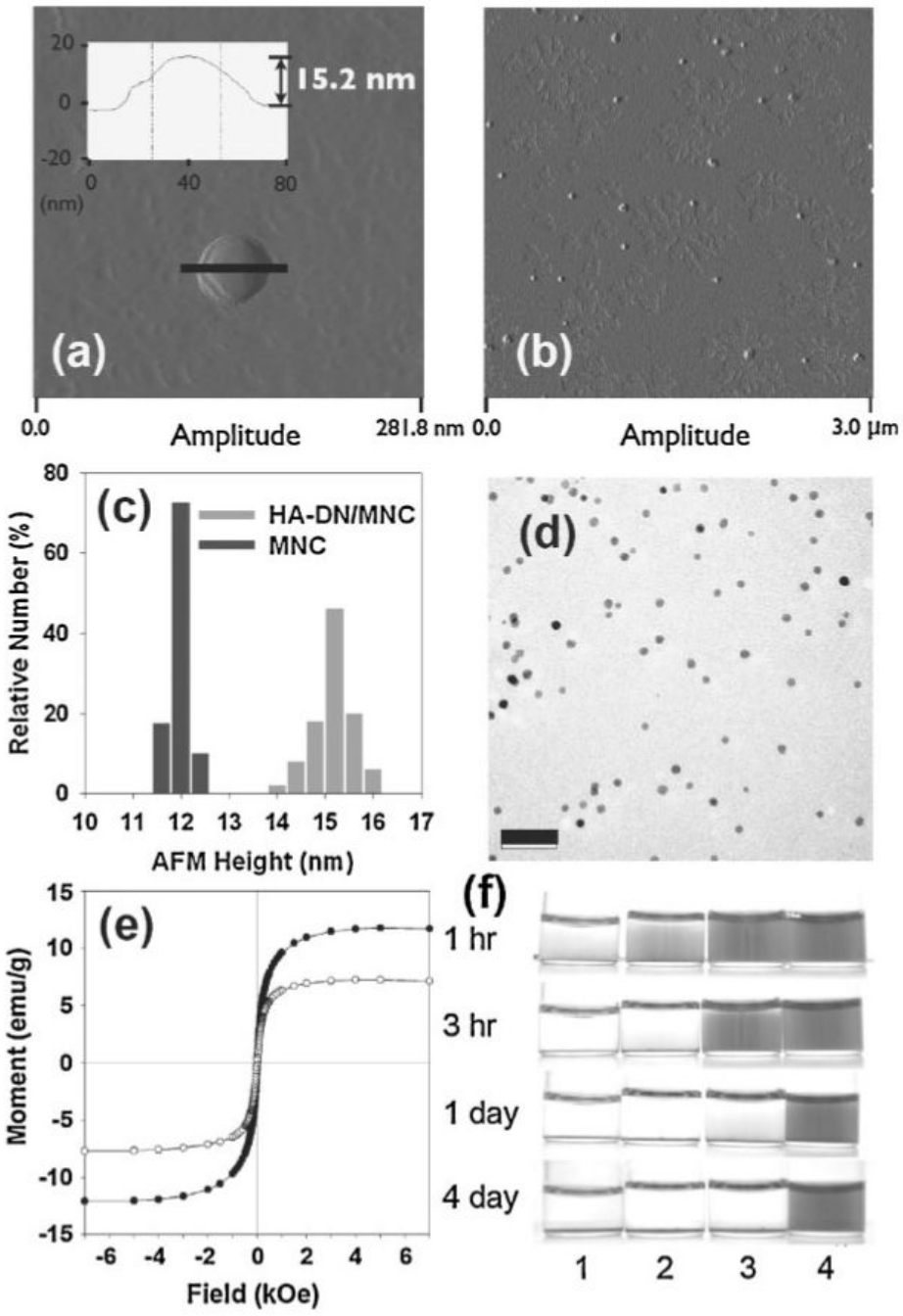

Figure 1.

a), b) AFM images of HA-DN/MNCs. (Inset: cross-sectional view of HA-DN/MNC through black line). c) Histogram of AFM height distribution of HA-DN/MNCs and as-prepared MNCs. d) TEM images of as-prepared HA-DN/MNC, showing well-dispersed nanoparticles. The scale bar is 100 nm. e) Field-dependent magnetization of CTAB-stabilized magnetic nanocrystals (black dots) and HA-DN/MNC (hollow dots) using SQUID. f) Photographic images showing time-course stability of HA-DN/MNCs: CTAB-stabilized MNCs in water (**1**), in HA solution (**2**), in HA-DN-L solution (HA-DN1/MNC) (**3**), and in HA-DN solution (HA-DN2/MNC) (**4**).

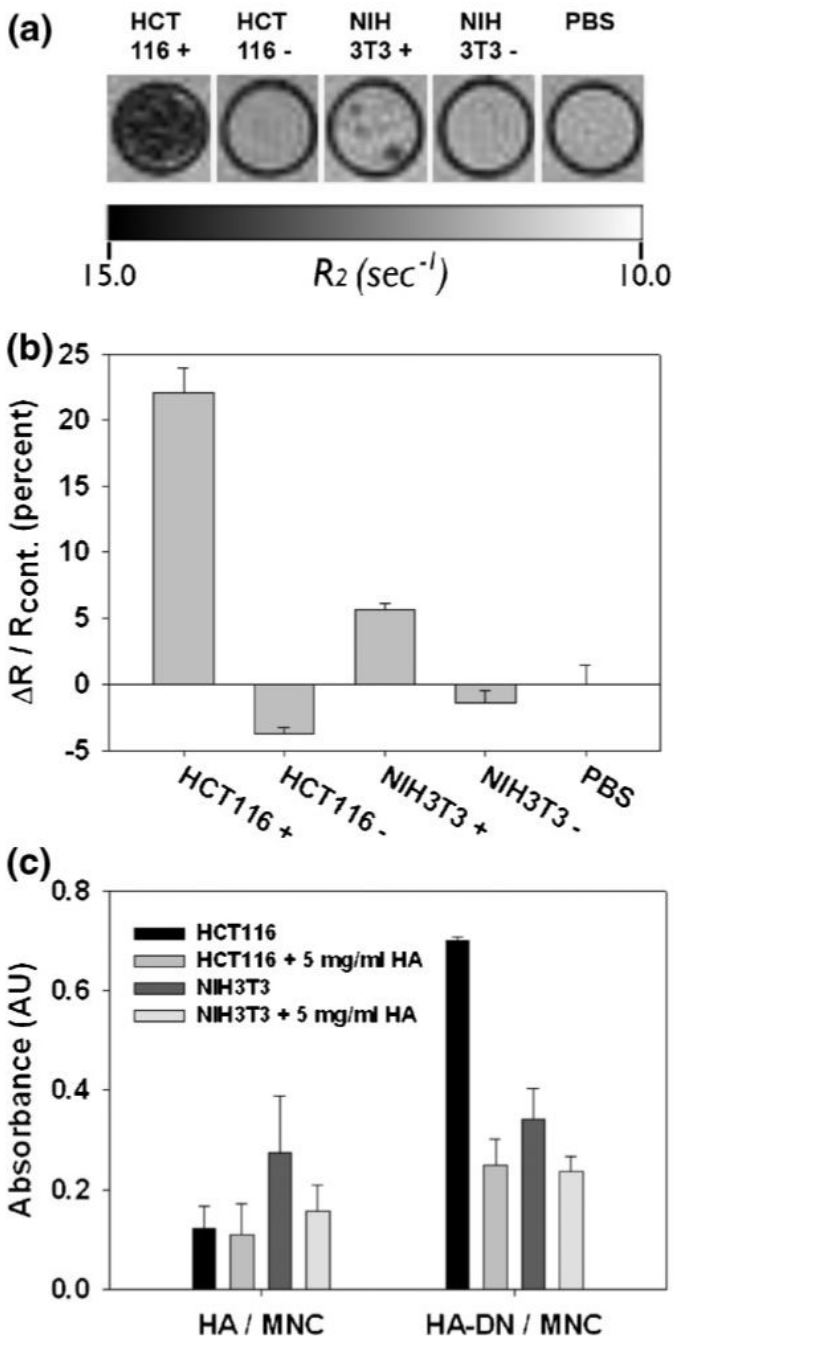

Figure 2.

a) T_2-weighted MR images and their color map for HCT116 and NIH3T3 cells. (**HCT116+**: HA-DN/MNC treated cells, **HCT116-**: control HCT116 cells, **NIH3T3+**: HA-DN/MNC treated cells, **NIH3T3-**: control NIH3T3 cells). b) Relative relaxation rates (R_2) ($\Delta R_2/R_{2cont}$, $R_2 = T_2^{-1}$) of cells. R_{2cont} is R_2 of PBS. c) Competition assays for cellular uptake of HA-DN/MNC using Prussian blue method.

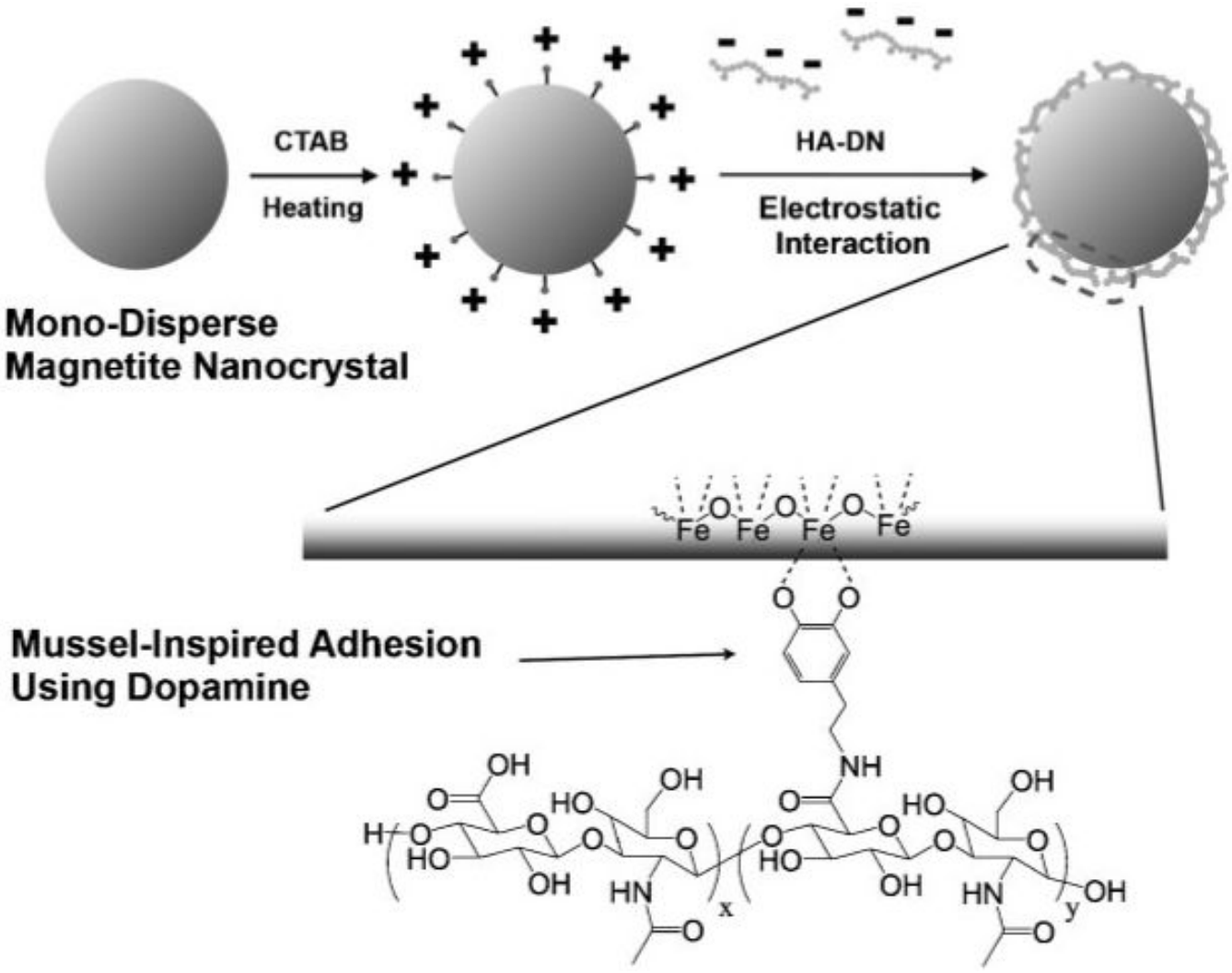

Scheme 1.
Synthetic procedure for homogeneous immobilization of HA-DN on a monodisperse magnetite nanocrystal (HA-DN/MNC).